

# Statistical Analysis of Wave Energy Resources Available for Conversion at Natural Caves of Cape-Verde Islands

WILSNON MONTEIRO<sup>1</sup>, ANTÓNIO SARMENTO<sup>2</sup>, ANTÓNIO FERNANDES<sup>1</sup>, JOAQUIM FERNANDES<sup>1</sup>

<sup>1</sup>Faculty of Science and Technology, University of Cape-Verde, Campus do Palmarejo, 279C – Praia Cape-Verde

<sup>2</sup>Lisbon High Technical Institute, Technical University of Lisbon, Alameda Campus, CP 1049 -001-Lisbon, Portugal

wilson.monteiro@docente.unicv.edu.cv

*Abstract:* - Using the time-series of significant wave height and the peak period between 1979 and 2009, generated by SOWFIA - Streamlining of Ocean Wave Farm Impact Assessment, some relevant statistical information about energy content available in ocean waves in Cape-Verde is obtained. The monthly and annual-average time-series of the average power are analysed and the confidence intervals for their values are defined. Considering all of the 31 years of data, the results show that the most energetic month, from the average power point of view is January (23.49 kW/m) and the least energetic month is July (15.04 kW/m). In fact, the monthly average power decays from January to July and increases from July to December (21.21 kW/m). The annual-average power for the 31 years of data exhibits a weak attenuation caused by data aggregation. However, using the moving average smoothing curve it is possible to note that, between 1999 and 2009, the values of annual-average power seem to stabilize around 18 kW/m. Using the appropriate Autoregressive Integrated Moving Average (ARIMA) model we verified that the future values of the annual-average power tend to oscillate around the same level of average power (18 kW/m). The outliers present in time-series of annual average power were identified and their influence in the value of annual-average power was quantified. Removing outliers from the annual time-series of power caused a maximum relative attenuation in the values of the annual-average power between 1.85 and 13%. Through the Coefficient of Variation of Power (COVP), obtained by dividing the standard deviation of the power time-series by the average power, it is possible to conclude that the wave resource is stable, with COVP between 0.46 and 0.66. The values of the Monthly Variation Index (MVI), the maximum range of the monthly mean wave power relative to the yearly mean level, show that the resource is relatively stable, with MVI < 1.2. The present work calculates the deep water power available for the Natural Caves (NC) in Cape Verde Islands, through a rigorous analysis of the wave climate that excites them. The minimum sampling size and the corresponding numbers of days of measurements per month in order to quantifying the output power from NC are also estimated. The results show that the required number of days of measurements is lower in spring (March to May) and summer (June to August). This is due to the lower level dispersion of wave data for these seasons, in comparison with the rest of the months.

*Key-Words:* - Wave Energy; Resources Characterization; Natural Caves; Statistical Analysis; Cape-Verde.

## 1 Introduction

Ocean waves constitute one of the renewable sources of energy that are gradually entering the market of clean and sustainable energy worldwide. The global theoretical energy from ocean wave is estimated in 17500 TWh/year [1]. Many countries around world have been investing on this natural resource to produce useful and sustainable energy. Portugal (Pelamis and Pico Plant Projects), Australia (CETO and OCEANLIX projects), France (SEAREV project), UK (OYSTER WEC and

Limpet projects) and Holland (AWS project) are examples of some countries that have recognized the feasibility of harvesting this source of energy [2]. According to the International Renewable Energy Agency [3], around 64 % of the Wave Energy Converters (WECs) has been projected for offshore application and 36% for near-shore and onshore operation. Some full-scale operational tests have been realized. These include the OYSTER device from Aquamarine Power, the Wave Roller from AW-Energy, Pelamis P2 from the Pelamis Wave

Power, the Seabased and the Sea-Tricity devices. Magagna (2011) [4] has identified, in 2011, over 100 wave energy developers. Yet, EMEC (2014) [5] has listed 170 wave energy developers worldwide. About 45% of the wave energy developers are based in or are currently developing projects in the European Union (EU) regions. The global installed capacity of wave energy remains low and the technologies are still at an advanced R&D stage. Just a few machines have sustained long operational hours, such as the Aquamarine OYSTER (>20000 hours) and Pelamis (cumulative > 10000 hours) [6]. The growth of the wave energy sector is lower than expected and this fact may affect the confidence of investors in this area. Success in attracting future Original Equipment Manufacturer investments will depend on the capacity of the developers in improving performance, reducing cost and validating wave energy technologies. The long-term global wave energy is expected to become cost competitive and provide an alternative to other Renewable Energy Sources and conventional energy resources. Through a review of the existing data available, the different cost components in the Capital Expenditure (CAPEX) estimate for wave energy extraction have been identified as follows (Table 1):

Table 1 :Costs components estimate for wave energy extraction [7]

Civil and Structural costs	38%
Mechanical Equipment costs	42%
Electrical and I&C supply and installation costs	8%
Project indirect cost	7%
Development cost	5%

Thus, the main components of CAPEX are mechanical equipment, civil and structural costs. In this context, the developers of wave energy technologies must undertake efforts and strategies aimed at reducing the two above mentioned costs and the risks associated with the operation of these equipments offshore or close to shore.

### 1.1 Natural Caves

Natural Caves (NC) are caverns formed naturally under the rocky shorelines, inside of which there is an air layer (Fig.1). This air layer acts like an air pump against the cave ceiling, as the wave enters and exits these natural infrastructures, forcing the compressed air to go in and out of the NC, through surface holes at the top of the cave. Fig. 2 shows NC with one and two holes.



Fig.1. Activity in a Natural Cave.



Fig 2. Activity in a Natural Cave with two holes.

The principles of NC operations are similar to the man-made Oscillating Water Column (OWC) device, projected for onshore application. Justification for using the NC for wave energy conversion is a possible cost reduction on the Civil and Structural cost components, which, as mentioned before, are the most significant costs associated with building wave energy devices to produce electricity. Furthermore, the risk of the device collapsing is minimized, by taking advantage of the sturdiness of the natural rocky structure, time tested by the waves and storms. To evaluate the potential of NC for electricity production, it is necessary to estimate its output power. To do this, a set of experiments aimed at determining the values of some important physics parameters of NC operations need to be conducted.

Monteiro and Sarmiento (2015) [8] carried out the analytical modelling of the NC operations as a function of their functioning physical parameters. The present study is part of a deeper work aimed at quantifying the output power of NC and to project an adequate power take-off system to be adapted on their holes, for energy extraction.

Since the excitation waves are irregular, non-linear and non-stationary phenomenon it is very important to determine beforehand the sampling size, i.e. how long it takes to carry out the experiments (number of days of measurements) on a Natural Cave, in order to guarantee the time representativeness of its output power. To achieve this goal, some statistical analysis has to be carried on the wave energy input regime.

## 2.2 Wave Energy in Cape-Verde: the state of the art

Cape-Verde is an archipelago of ten islands in the Atlantic Ocean, off the West Coast of Africa, with roughly half million people. The country is totally dependent on oil to produce electricity, having one of the most expensive cost of electricity in Africa, around 0.28 Euro/kWh [9] versus 0.17 Euro/kWh [10] at Senegal, a continental neighbour. Some investments were made by the Government of Cape-Verde aimed to introducing renewable sources of energy in the country, mainly solar and wind energy. The Renewable Energy Plan for Cape-Verde (ERPCV) has defined an ambitious goal of achieving 50% of Renewable Energy penetration in the country by 2020 [11]. As a results of the ERPCV, there are in the country four wind energy farms with a total annual production between 80 and 110 GWh and two solar energy farms with 7.5 MWp (MWp- Mega Watt Peak) [11]. In 1999, some research projects on ocean energy were initiated in the country, directed at Ocean Thermal Energy Conversion (OTEC) system and WaveStar technology (Wave energy). Unfortunately, these projects did not produced any visible results since they lacked a institutional framework on which to develop.

Because of its insular nature, most of Cape-Verde's economic activities (around 90%) are concentrated on coastal areas [12]. In this context, it makes sense to use wave energy for producing electricity locally. A clear alternative is harvesting the energy from ocean waves. The evaluation of the wave energy resources and the feasibility associated with its utilization in Cape-Verde need to be assessed in more detail. Before 2009, some pilot projects for wave energy conversion at south coast of Santiago

Island were conceived but never implemented and worst yet, never went beyond pre-feasibility studies [13]. In 2009 an attempt was made to deploy the WaveStar device, developed by Danish company WaveStar Energy, at Sal Island. This project forecasted the wave energy resources in some regions around the Island, using measurements gathered by a wave buoy installed in place. Unfortunately, the project failed to achieve its goals and the buoy was abandoned at the Instituto de Meteorologia e Geofisica de Cabo-Verde, in Sal Island [13]. In 2011, GESTO Energy, a Portuguese company, carried out an evaluation of the wave resources in Cape-Verde based on eleven years of data produced by meteorological wave model worldwide. The data of direction, period and significant wave height were characterized and the values of these parameters were used for calculate the offshore annual average wave power [11]. According to this study, the islands that present the best potential for wave energy exploration are Sal, S. Antão, S. Vicente and Boa Vista. In fact, four projects for offshore wave energy conversion based on the Pelamis technology were proposed for these islands (GESTO, 2011): Sal (3.7 MW), S. Antão (3.7 MW), S.Vicente (3.7 MW) and Boavista (3.5MW). The study was commissioned by the Ministry of Turism, Industry and Energy of Cape-Verde and, unfortunately, the scientific results of the study are unknown since it was never published in any scientific journal or conference proceedings.

As there are no scientific data available on wave energy resources for Cape Verde Islands, the present work brings to light the real potential for wave energy harvesting and constitutes a significant contribution to authorities on which to base any decision about forthcoming investments on wave energy conversion. However, more detailed information will be needed in order to accurately validate the result of this study, as will be shown in next section.

The characteristics of wave such as its slow and reciprocating motion, its high instantaneous power fluctuation level, the occurrence of extreme environment requires machines that absorbs high loads in multiple directions and structures that withstand extreme loads in storms [14]. These characteristics of wave power forces the Wave Energy Converters (WEC) to be large and costly in comparison with their level of energy output. So, to prevent the high cost of WEC projects it is important to avoid their oversizing. In this context, the correct evaluation of the nature of the available power in waves is very important. The methodologies we propose in the present paper

consist in analyzing the nature of the time-series of power data to help us quantify more accurately the available power for conversion at WEC. In fact, the calculation of temporal representativeness of the wave power data to be used for evaluation of the energetic performance of a NC could be adapted for all WEC. The identification of outliers, observations that lie at an abnormal distance from others values in a random sample from a population, helps to avoid the oversizing of the WEC and therefore lowers the project cost. In fact, if the occurrence of this extreme event is insignificant the project of the power take-off system must be rethought. The durability of the WEC is another aspect that bothers anyone interested in this area. The ANACONDA device is made using rubber tube that resist the extreme wave conditions [15]. The Natural Caves, described in the present work is meant, on one hand, to augment the durability of an OWC (Oscillating Water Column) WEC using the natural structures, tested by time and storms and, on the other hand, to diminish the civil cost associated with the OWC WEC.

The procedures and software available for mapping wave energy resources ignore, in general, some important statistical aspects that can lead to errors in wave energy assessment. The outliers that may be present in the time-series of wave data, as a result of a specific event such as extreme storms, could significantly influence the available average wave power. Yet, as the experimental study carried out by Mendes and Monteiro (2007) [16] shows, some inshore WEC such as the OWC device, present serious handicaps when operating in high waves since these waves produce significant hydrodynamic loss associated with the interaction between waves and the caisson structure. Thus, the present study introduces a novelty by using adequate statistical tools to identify possible outliers in time-series of wave data, and the subsequent analyses of their influence in the annual-average power calculation. Another subject barely mentioned in papers, that can lead to error in the wave energy resources characterization are the effects of data aggregation. The information about the temporal behaviour of the wave data are lost due to the aggregation effects. The present study shows that the aggregation effects may be a real problem that deserves to be taken into account when characterizing wave energy resources. Finally, based on the wave regime characteristics, this paper calculates the time duration necessary to carry on the experiments at Natural Caves aimed to quantify their output power with a minimum sample size that will guarantee its time representativeness. The estimation of the time duration is very

important as it helps evaluate correctly the energetic performance of NC. In fact, the statistical procedure presented in this paper for quantifying the time duration can be followed by other researchers to better understand the behaviour of their models of wave energy devices.

## 2 Data

Knowledge of wave energy resource at a certain location is required by developers of Wave Energy Converters projects in order to allow them to select the most favourable sites for achieving optimal power capture and economic performance from their devices. Three main categories of data are available for wave energy resources assessment: In-situ measurements (buoy, pressure transducers, wave staff, ship-borne wave recorders), remote sensing (satellite radar Altimetry RA, Synthetic Aperture Radar SAR, Marine Wave Radar), numerical models for deep-water (WAM and WaveWatch 3) and for shallow-water (SWAN, TOMAWAC and MIKE21).

SOWFIA-Streamlining of Ocean Wave Farm Impact Assessment is an EU Intelligent Energy Europe Project with the goal of sharing and consolidating pan-European experience and best practices for consenting processes and environmental and socio-economic impact assessment (IA) for offshore wave energy conversion developments [17]. This project brings together ten partners across eight EU Member States actively involved in planned wave farm test centres and aims at providing recommendations for streamlining of IA approval processes with the purpose of removing legal, environmental and socio-economic barriers associated with development of the wave energy farms. The SOWFIA project uses data obtained from direct measurements (wave buoy) of the wave climate, carried out at the seven European wave energy test centres, through the Data Management Platform (DMP) tool. DMP is an interactive tool designed to assist in the decision making process, providing information on different wave energy monitoring activities at different test centres and allowing direct visualization and downloading of relevant data. The DMP is publically available on the SOWFIA website. The seven European test centres involved in the SOWFIA project are the AMETS (Ireland), BIMEP (Spain), Lysekil (Sweden), Ocean Plug (Portugal), SEAREV (France), Wave Hub (United Kingdom) and EMEC (Scotland) [17].

For others regions of the ocean, where there are no in situ data measurements, the SOWFIA project

uses data produced by WaveWatch 3 (WW3) wave model. The WW3 is phase-average model that solves the spectral action density balance equation for wavenumber-direction spectra. The Governing equation includes refraction due to the temporal and spatial variation of the mean water depth and current. The source terms include nonlinear interactions, dissipation due to the white capping, bottom friction, wind wave growth and decay [18]. An important constraint of the formulation of the WW3 is that the parameterizations of the physical process included in the model do not address conditions where the waves are strongly depth-limited. This constraint implies that the model is generally applied on spatial scales between 20 and 100 km outside of surf zone (Tolman, 1999).

Like other sources of renewable energy, the nature of ocean waves is complex and impossible to be predicted precisely. The data produced by WW3 model must be, wherever possible, calibrated with in situ measurements using wave buoy or altimeter data. Both calibrations of the wave data and the estimation of the confidence bounds are made difficult by the complex structure of errors in the model data. Error in parameters from wave model show nonlinear dependence of variety of factors, seasonal and inter-annual changes in bias and short-term temporal correlation [19]. To assess the uncertainty associated with the estimation of energy yield from a wave energy converter (WEC), Mackay et al (2010) use two hindcasts from European Marine Energy Centre in Orkney. These hindcasts are produced by WAM [20] and WW3 wave models and calibrated using a Datawell Directional Waverider buoy moored in 50 m water depth at the EMEC site. The study show that before wave data calibration, the estimation of the long-term mean WEC power from the two hindcasts differ by around 20%. After calibration this difference is reduced to 5%.

Data produced by WW3 through the SOWFIA project is used to evaluate the wave energy resources at Cape-Verde. The data was gathered for period between 1979 and 2009, at coordinates 16°N-24°W, approximately at centre of the archipelago, where the water depth is around 3.7 km [21]. The WW3 produced information about the significant wave height ( $H_s$ ), peak period ( $T_p$ ), peak direction ( $D_p$ ) and wind velocity, every 3 hours. The data generated by a wave model, should have been calibrated against data collected in situ, but unfortunately, there is no in-situ calibration buoy in the region. Another factor which introduces some inaccuracy in the data, is the shadow effect caused by the own presence of the islands. According to

Ponce de Léon et al. (2010) [22] the shadow effect is not taken into account in wave models and can introduce inaccuracy in wave data, especially at the location where the wave regime is characterized by low values of  $H_s$ . Another important aspect that deserves mentioning is the location of the Natural Caves (inshore) relative to the location of the data acquisition (offshore). Further study on the wave transformation from deep to shallow water must be carried out using information about the local bathymetry. Unfortunately, detailed bathymetric data is only available for some bays and harbours. Therefore, further approximations of coastal bathymetry must be made in order to obtain a more realistic result of wave energy resources available at shorelines regions.

### 3 Methodology

Calculation of the wave energy input regime is carried out using principles and parameters described below.

#### 3.1 Average Power

In deep water, where the depth is greater than a half of the wavelength, the average wave power can be determined through the following equation, applied only for unidirectional wave spectrum approximation.

$$P = \frac{\rho g^2 H_s^2}{64\pi} \quad (1)$$

Where  $H_s$  is significant wave height,  $T_e$  is energy period, defined in terms of the spectral momentum by the following relations:

$$H_s = 4m_0^{1/2} \quad (2)$$

$$T_e = \frac{m_{-1}}{m_0} = \frac{\int_0^{2\pi} \int_0^\infty f^{-1} S(f) df d\theta}{\int_0^{2\pi} \int_0^\infty S(f) df d\theta} \quad (3)$$

in which,  $m_{-1}$  is the spectral moment of order -1,  $m_0$  is the spectral moment of order 0,  $f$  is the frequency,  $S(f)$  is the spectral density function and  $\theta$  is the direction of the energy propagation [23].

The characterization of the wave climate is made by the combination of the significant wave height  $H_s$  and peak period  $T_p$  or the zero-crossing period  $T_z$  parameters. The energy period determined by the Eq.(3) require the knowledge of the form of energy spectrum. When the form of the energy spectrum is

unknown it can be approximated by any of the many model available [23]. This is the approximation used for the Marine Atlas of Renewable Resources in UK [2]. Another approximation commonly used for  $T_e$  is represented by  $T_e \approx \alpha T_p$ , where  $\alpha$  is an empirical parameter. The approximation  $T_e = T_p$  used to evaluate the wave resource for Cape-Verde was considered, by Hagerman (2001) [24], very appropriate to make a preliminary analysis of wave energy resource. Using the monthly series of the available power in waves it is possible to define the annual time-series of this parameter through the following expressions:

$$P_{aj} = \frac{\sum_{i=\text{initial month}}^{\text{initial month}+11} P_{ij}}{12} \quad (4)$$

In the above equation  $P_{aj}$  is the average power for year  $j$ ,  $P_{ij}$  is the average power for the month and year. In this way, the monthly time-series begin on January and ends on December of each year.

It is important to note that there is no physical justification for wave power to be monthly periodic, but since the sun-cycle is the underlying cause for atmospheric pressure distribution and wind patterns over the ocean, most likely it will be yearly periodic.

The reason to calculate monthly series of available power is just related to how data is collected and made available at SOWFIA.

### 3.2 Monthly Variation Index (MVI)

The temporal variability of the wave resources is a key factor that affects decisively the feasibility of wave energy projects. In this sense, the regions of the ocean where the resources are stable are more attractive for any possible investors. Naturally, the level of the average power is another important factor for viability of wave energy harvesting. The Monthly Variation Index is defined as the ratio of the differences between the maximum and minimum values of the monthly average wave power in year  $j$  by the corresponding annual average wave power [25]. That is,

$$MVI_j = \frac{(P_{\max} - P_{\min})_j}{P_{aj}} \quad (5)$$

where  $P_{\max}$  and  $P_{\min}$  are, respectively, the maximum and minimum values of the monthly average power in year  $j$ .

### 3.3 Coefficient of Variation of Power (COVP)

COVP is another very important parameter used to evaluate the temporal variability of wave resources. This quantity is defined by the ratio between the standard deviation of the wave power and the respective annual average wave power in year  $j$  [25]

$$COVP_j = \frac{\sigma(P(t))_j}{P_{aj}} \quad (6)$$

In the Eq.(6),  $P(t)$  is the values of power evaluated each 3h, represent the standard deviation of temporal series of wave power,  $P(t)$ , for year  $j$ , and  $P_{aj}$  is the respective annual average wave power. According to Cornett (2008) [25], small values of COVP mean that the wave resources are stable. For  $0.8 < COVP < 0.9$  the wave resources can be considered moderately instable. Therefore, for  $COVP > 0.9$  the resource is unstable.

### 3.4 Statistical analysis

The wave climate at a certain location is well characterized by the time-series of significant wave height and the peak period, which are recorded every 3 hour (time interval necessary for verifying significant change in wave spectrum). Using these parameters, other statistics such as the average available power in waves can be calculated. To understand the time-series behaviour of some important wave parameters, to calculate the confidence interval, the smoothing curves, and the forecast of its values, some statistical tools of analysis are used. In this context, some well known statistics software such as R software [26], gretl software [27], XLSTAT [28] and Minitab [29] are used. Aspects such as the trend analysis, stationarity and normality tests of the average power are here analysed. To perform the forecast of the average power in waves, the Autoregressive Integrated Moving Average (ARIMA) model is used. Non-seasonal ARIMA model is generally represented as ARIMA (p,d,q) where,  $p$  is the order of the Autoregressive Model,  $d$  is the degree of differencing and  $q$  is the order of the Moving Average Model [30].

Finally, the most common sea-states in Cape-Verde can be shown through the wave histogram. The wave histogram is a table that lists the occurrence of the sea-states in terms of significant wave height and peak period or mean up-crossing period. It is the long-term statistical representation of sea states. Using the information in the wave histogram it is



possible to identify the most common sea states in a certain region.

### 3.5 Representativeness of the monthly average output power from the NC

The energy that excites the NC is a function of the local wave regime, while its output energy depends on the input energy (wave regime) and on the geometry of the NCs (Fig. 3). For each Natural Cave the geometry is fixed, hence the output energy is directly determined by the local wave regime. This means that the variation in the output energy content is caused by the variation in the input energy content, that is by the variation of the local wave regime. In this context, it is reasonable to assume that the minimum sampling size necessary for characterizing the input energy content is equal to the minimum sampling size needed to characterize the output energy from the NC. The calculation of the minimum sampling size for characterizing the input energy into the cave is done using the Minitab Software. For three hours time interval between successive readings, the total number of data points acquired during one day is eight. So, if this minimum sampling size is represented by  $N_{in}$ , the correspondent minimum time duration for data acquisition to achieve the representativeness of the input power is  $N_{in}/8$  days. Therefore, to guarantee the representativeness of the output energy from the NC the duration necessary to realize the experimental study on these natural infrastructure is equal to  $N_{in}/8$  days.

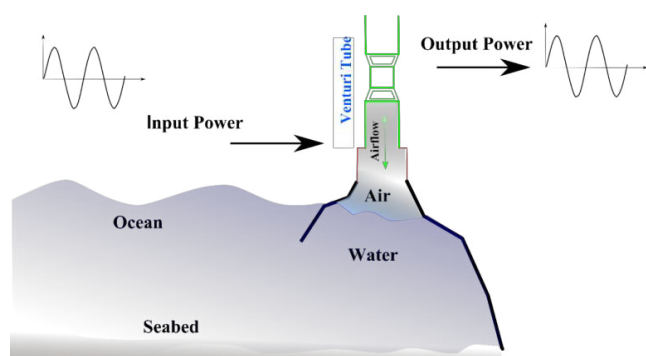


Fig. 3. Energy production system by NC.

## 4 Results

Table 2 (appendix) shows the histogram of wave regime, where 78.03 % of the waves have significant wave height of 1-2 m and 20.81% of all occurrences feature peak period from 6-9 s and significant wave height from 1.5-2 m. The minimum and maximum values of significant wave height and peak period recorded are, respectively 0.59 m and

3.82 m and 2.85s and 22.12 s. Yet, the histogram presented in Table 2 shows two local maxima for the peak period 6 to 9s and 12 to 15s, for significant wave height between 1.5 and 2.5 m. This bimodal distribution indicates a superposition of two distinct wave regimes. According to Holthuijzen (2007) [31], the spectrum at a prediction point is the superposition of waves from all directions, accounting for all processes of generation. The wave regime can be classified into wind-sea and swell, the latter when the peak period waves have phase velocity higher than the wind speed and are capable of propagating outside the generating area. Analysis of wind-sea and swell fields for mid-latitude and tropical Atlantic for the period 2002–2008 using a combination of satellite data (altimeter significant wave height and scatterometer surface winds) and model results (spectrum peak wave period and propagation direction) done by Farias, et al. (2012) [32], shows a dominance of swell over wind-sea regimes throughout the year in the Atlantic. Fig.4 shows the wave rose diagram obtained for these two wave regimes. The first diagram (A) represents the predominant direction for peak periods between 6s and 9s. These waves are generated by the predominant winds, blowing constantly throughout the year, from NNE direction. Since there is not enough fetch length between Cape-Verde Islands and the African continent (600 Km), the wave regime do not fully develop and remains with a peak period between 6 and 9 seconds.

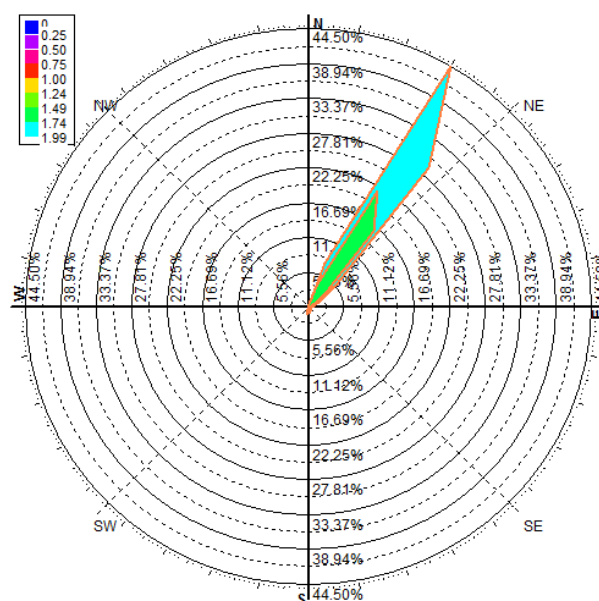


Fig. 4A Wave rose for local maxima characterized by the peaks periods between 6 and 9 s.

The second diagram (B) represents the predominant direction for peak periods between 12s and 15s and shows a superposition of waves from two origins:

- NNW waves which are generated during early-year winter storms in the North-Atlantic.
- SSW waves which are in turn generated during the end-year autumn storms in the South-Atlantic.

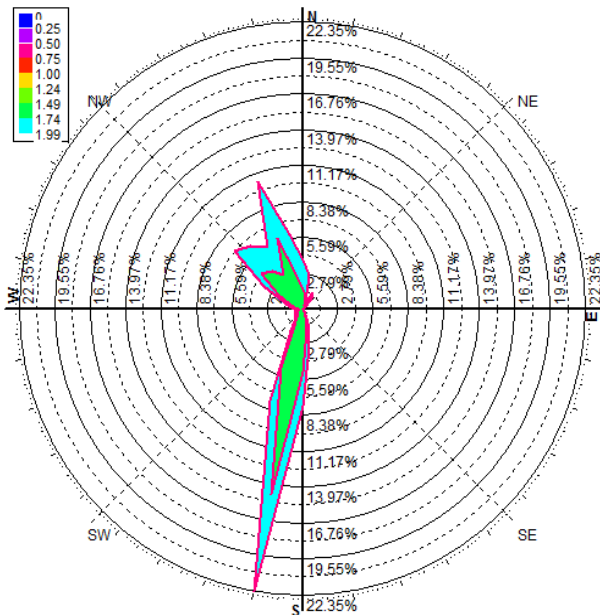


Fig. 4B. Wave rose for local maxima characterized by the peaks periods between 12 and 15 s.

Both regions have sufficient fetch length to fully develop the wave regime, and there are outliers of 17s – 18s generated in South-Atlantic.

This is consistent with later findings in this paper that January and December are the most energetic months and July is the least energetic month.

### 4.1 Seasonality and trends

The curves on Fig. 5 show no clear trend on the time-series of the monthly average power, over the years. This fact is confirmed by the Mann-Kendal test [33] whose results are presented at Table 3 (appendix). The Mann-Kendal test (at 5% level of significance) was done using commercially available software [28]. The results show that these monthly time-series can be considered trendless over the years, except for September and October with low p-values of 3.8% (September) and 1.8% (October). However, these trends may be the results of data aggregation error that will be reported in more detail later in this work.

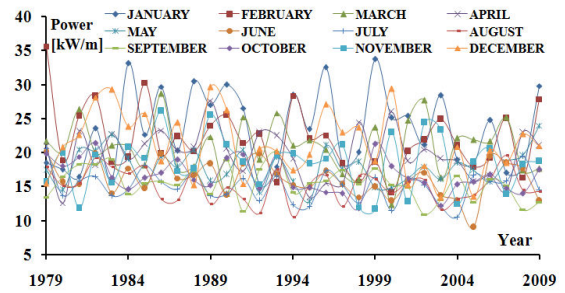


Fig.5 Time-series of monthly average power.

Fig. 6 shows the minimum, average and maximum power available on waves which has been calculated for each month of the 31 year long record. The graph clearly shows that the most energetic month is January (23.49 kW/m) and the least energetic month is July (15.04 kW/m). In fact, the average power decays from January to July and increases from July to December (21.21 kW/m). The curves show, as may be expected, winter power exceeding summer power as is the case region off the north coast of Scotland [19].

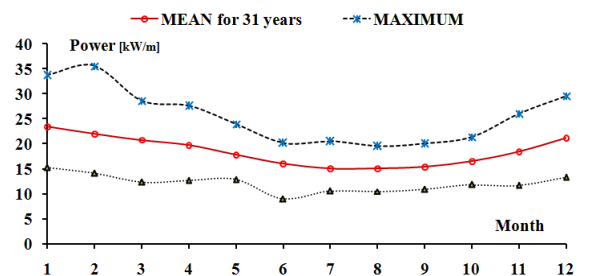


Fig. 6 Statistics of monthly average power for 31 years of data.

Fig.7 shows the annual-average values of significant wave height ( $H_{sav}$ ) and peak period ( $T_{pav}$ ), together with their moving average smoothing curves (MASC) of seven periods [34]. According to this figure, the maximum and minimum annual-average values of the significant wave height are equal to 1.83 m and 1.61 m, recorded, respectively, in the years 1986 and 1997/2005. After 1990, the annual-average values of the significant wave height shows a rapid decay until 1998, after which it shows a quasi-constant behavior around 1.68 m, until 2009. The annual-average values of the peak period has its maximum value of 11.00 s in 1997 and minimum of 9.91 s, in 2007. In general, the values of this parameter show a downwards trend over the years. However, due to the high variation of the power between 1994 and 1997 the smoothing curve shows an upward trend during this interval of time. After 2002 it shows a quasi-constant behaviour, around 10.5 s.



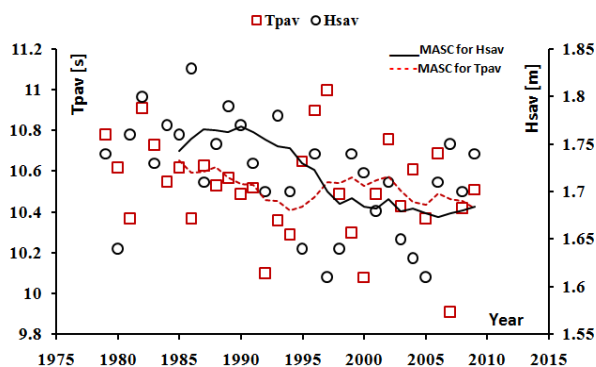


Fig. 7 Annual-average values of significant wave height and peak period.

The annual-average values of power available in waves, Eq.(1), are shown in Fig.8. The maximum and minimum values of this parameter are 21.04 kW/m and 15.94kW/m attained, respectively, in 1982 and 2005. The annual-average values of power show a downward trend until 1998, after which it exhibits a quasi-constant behavior around 18 kW/m, until 2009.

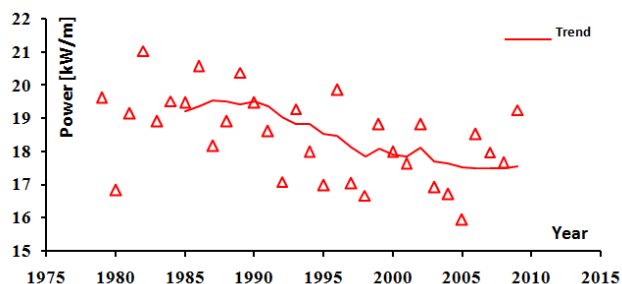


Fig. 8 Time-Series of annual-average power.

For a more in depth analysis of the trend of the annual-average power time-series the Augmented Dickey-Fuller (ADF) trend test was used. As the Fig.8 shows, the time-series of the annual-average power shows an initial downward trend and a constant, as its values oscillate around a nonzero constant. Thus, in the ADF trend test we assume that the power is the sum of a constant and a trend. Another aspect associated with the utilization of the ADF test is the calculation of the optimum Lag length. To do this, the calculation of the maximum Lag length ( $Lag_{max}$ ) is necessary. This can be done using the equation  $Lag_{max} = \text{int} \left\{ 12(T/100)^{1/4} \right\}$ , suggested by Schwert (1989) [35]. In this equation, “int” means that we must accept the integer parts of the results produced by the equation and T is the dimension of sample. For our case study,  $T=31$  (for annual-average time-series) observations and, therefore, the  $Lag_{max}=9$  Using the function “Var Lag” in gretl software, it is possible to calculate,

automatically, the optimal Lag length, according to Akaike Information Criterion (AIC), Bayesian Information Criterion (BIC) and Hannan-Quinn Information Criterion (HQC) [36]. The results produced by this procedure are presented in the following Table.

In Table 4 (appendix), “\*” means the best Lag length. Thus, the optimum Lag length is, then,  $Lag=1$ , according to all the criteria mentioned before. Using the gretl software for this optimal value of the Lag length and for the assumptions that the power is the sum of a constant and trend, as mentioned before, the ADF trend test produces a  $p\text{-value}=0.0001$  very low, in comparison with the level of significance ( $\alpha=0.05$ ) used to perform the test. Therefore, the null hypotheses of non-stationarity must be rejected. Thus, the time-series is stationary around a deterministic trend. That is, the annual-average time-series of power is a trend-stationary process [37]. This kind of trends is caused by a moving average component that is an explicit function of time. To better understand the nature of the trend, exhibit by the values of annual-average power, it would be worth to carry on the trend test of the original time-series of power. Fig.9 shows the original time-series of power, between 1979 and 2009 calculated for each 3h. Analyzing this figure becomes clear that the values of the power oscillate around a constant different from zero and there is no clear evidence of trend in the value of the referred parameter.

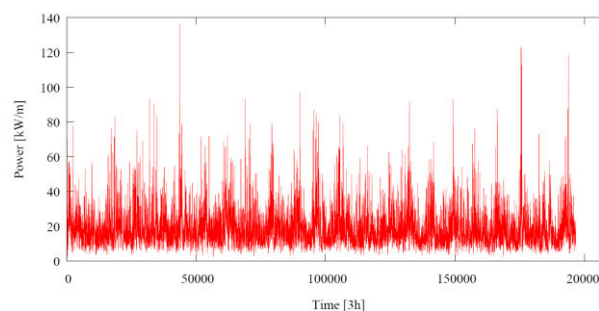


Fig. 9 The original time-series of power, between 1979 and 2009.

The optimum Lag length is calculated and is equal to  $Lag = 21$  (AIC),  $Lag = 7$  BIC and  $Lag = 9$  (HQC). These different results for optimum Lag-length could be associated with the heterogeneity of our data. The ADF test was carried out for all three Lag lengths and all of them produced a rejection of null hypothesis of non-stationarity. So, the original time-series of power is stationary around a constant mean. These results lead us to conclude that the initial trend shown in the values of the annual-average time-series of power could have been

caused by two factors: the effects of aggregation [38] and the existence of the Outliers, defined as an observation in data set which appears to be inconsistent with remainder of that set of data [39]. These outliers could affect significantly the mean values of power. According to Clark et al. (1976) [38], aggregation problem can be defined as the information loss which occurs in the substitution of aggregate, or macro-level, data for individual, or micro-level, data. This undesirable effect reduces the variability of data. In fact, aggregating the values of the power into its annual-average values produce, in our case, a reduction of standard deviation parameter from 10.39 kW/m, in original time-series, to 1.29 kW/m, in annual-average time-series. This corresponding to a dramatic reduction of 87.5% of standard deviation in comparison with the value of this quantity for the original time-series, and it could introduce a high level of error associated with the aggregation effects.

Defining a set of samples using all values of the significant wave height, peak period and the average power obtained for each month during the 31 years of data, the confidence intervals for all of these parameters were calculated, using the Minitab software and admitting a significance level of 5%. Before defining the referred confidence intervals the normality tests for all of these parameters were performed. Table 6 summarizes the statistical information about the normality tests, average values and confidence intervals for each month. The values of the A-squared parameter shows that the data is non-normal [40]. According to D'Agostino (1986) [40], the critical value of the A-squared parameter, for a 95% confidence level, is 0.752. The values of this parameter presented in Table 6 (appendix) are higher than this critical value. So, there is a very strong evidency that the data is non-normal. This result is confirmed by the p-values that are, in all cases, lower than 0.05 (significance level) implying the rejection of the normality hypothesis. The Minitab software has an option to calculate the confidence intervals for non-normal data. The results are presented in Table 6 (appendix).

## 4.2 Outliers

To analyze the implications of the outliers in our results, they were identified, through the Tukeys' method (Boxplot) [41], using, for the present study, the R software, and subsequently removed from the time-series. For identifying the outliers, this method uses the concept of the interquartile range to extract the very large and the very small values present in data set. The numbers

of the outliers found, in this way, for each year of the time-series, are presented in Table 5 (appendix).

As we mentioned before, all outliers are removed from the original time-series of annual average power. Further, the time-series of the annual-average power is, then, calculated, and the results are plotted in Fig.10, together with the correspondent annual-average power including outliers. As the referred figure shows, the trend-stationarity process persists even when removing the outliers. That is, the trend is not caused by the influence of outliers. But, they introduce a slight relative variation, between 1.85% and 13% in the values of annual-average power. However, at times of extreme storms, severe outliers may appear. In this context, it is worth analyzing the influence of these severe outliers in the context of wave energy resource characterization. Now, it is clear that the trend of the annual-average power is a result of data aggregation.

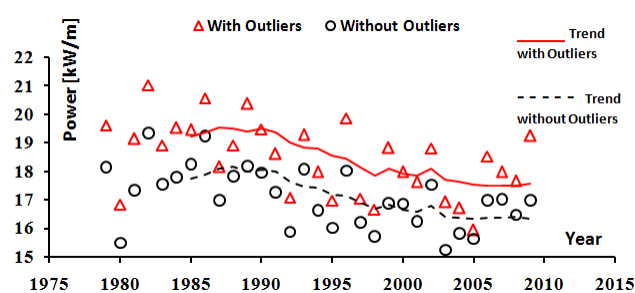


Fig. 10 The time-series of annual-average power, with and without outliers.

## 4.3 Projection

To estimate the future behaviour of the values of the annual-average power a forecast for the next 10 years is performed. For this purpose, it is necessary to calculate the best ARIMA model.

According to the ADF trend test, the time-series of the annual-average power is trend-stationary. The first difference (P-1) is stationary as it is possible to see through the values of the Autocorrelation Factor (ACF) and of Partial Autocorrelation Factor (PACF) presented in Fig.11, generated by gretl software. In fact, as shown in Fig. 11, the values of these parameters are statistically equal to zero, as they are less than 0.35, after Lag = 1 (for ACF) and Lag = 2 (for PACF). ACF and PACF are two statistical measures that show how the observations in a time-series are related to each other. Thus, to determine a proper model for a given time-series, it is necessary to carry out the analysis of these parameters [42]. In the present case, the original time-series is

converted into stationary time-series after the first differencing ( $d = 1$ ).

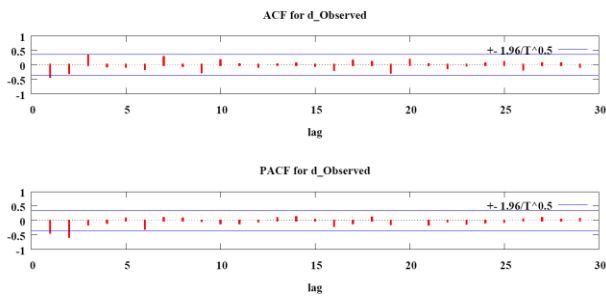


Fig. 11 The values of ACF and PACF parameters for the annual-average power time-series.

According to Hintze (2007) [43] the value of  $p$  is determined from the PACF of the appropriate differenced time-series. If the PACF cuts off after a few Lags, the last Lag with a large value would be the estimate for  $p$ . Therefore,  $p$  is equal to 2 (Fig.11). The value of  $q$  is estimated, following the same procedure, using the values of the ACF parameter shown in Fig.11. So,  $q=1$  and, the best ARIMA model to make the forecast is ARIMA (2, 1, 1). However, using the R software it is possible to generate automatically, the best ARIMA model to make a forecast of a time-series. For our annual-average power time-series the R software produce the ARIMA (2,1,0). According to AIC and HQC criteria the ARIMA model generated by R software is better than ARIMA (2,1,1). In fact, the ARIMA (2,1,0) led to the lower values of AIC (103.78) and HQC (105.57) in comparison to which presented by ARIMA (2,1,1) that were, respectively, 104.83 for AIC and 107.07 for HQC. Thus, in the present study, the forecast was made using the best ARIMA model, that is the ARIMA (2,1,0).

Fig.12 shows the results of the forecast for the annual-average power, achieved using the gretl software. As Fig.12 shows, the predicted time-series follows the observed time-series and produced a residual values that oscillate around zero (Fig.13), which shows that the predicted values tend to adjust to the observed values. According to the forecast, the predicted time-series of the annual-average power seems to oscillates, without any trend, around of 18 kW/m, as was previously predicted using the moving average smoothing curve. This value is very close to the one calculated by Falnes. J. (2007) [44], for tropical regions, similar to Cape-Verde Island. However, the uncertainty about the forecast is high. The Confidence interval spans a wide range of annual-average power.

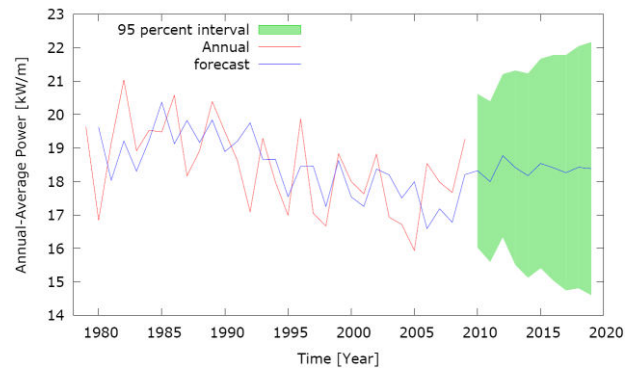


Fig.12 Forecast of annual-average power (generated by gretl software).

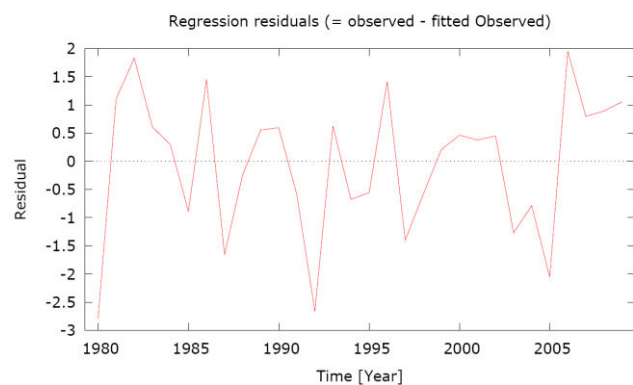


Fig.13 Residual values of the forecasted annual-average power time-series (generated by gretl software).

The normality test of Anderson-Darling [45] shows that the annual-average power follows a normal distribution with  $p$ -value equal to 51.5% (Fig. 14). As this  $p$ -value is higher than the significance level of 5%, the hypothesis of the normality distribution is accepted. Fig.14 was generated by Minitab software and represents a summary report of the annual-average power time-series. It shows, with a significance level equal to 0.05, the confidence intervals for the annual mean (17.981 kW/m – 18.924 kW/m), for the annual median (17.879 kW/m – 19.186 kW/m) and for the annual Standard Deviation (1.028 kW/m – 1.719 kW/m). Fig. 15 shows the normal probability plot for the annual-average power. As it is possible to note in this figure, in general, the data follow the normal line. However, some deviation from this normal line is registered between 16.99 kW/m and 17.09 kW/m.

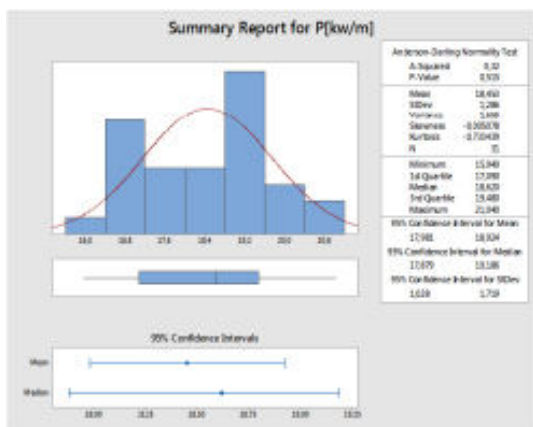


Fig. 14 Summary report of annual-average power, between 1979 and 2009.

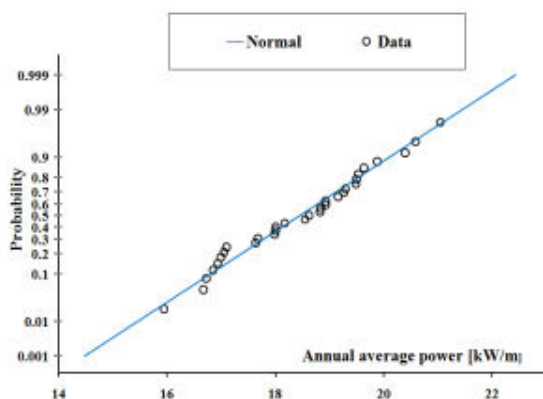
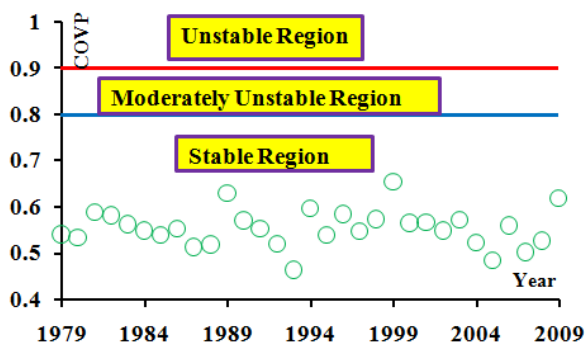


Fig. 15 Normal probability plot.

**4.4 Stability**

The wave energy resources in Cape-Verde are stable with COVP less than 0.8, as it is possible to see in Fig. 16-A, which represents the time-series of the annual values of COVP. The MVI parameter shows that the monthly wave energy resources can be considered relatively stable with MVI values less than 1.2 (Fig. 16-B). This is a very attractive aspect associated with the utilization of wave energy to produce electricity in Cape-Verde, since it affects the useful life cycle of ocean wave conversion equipment.



(A)

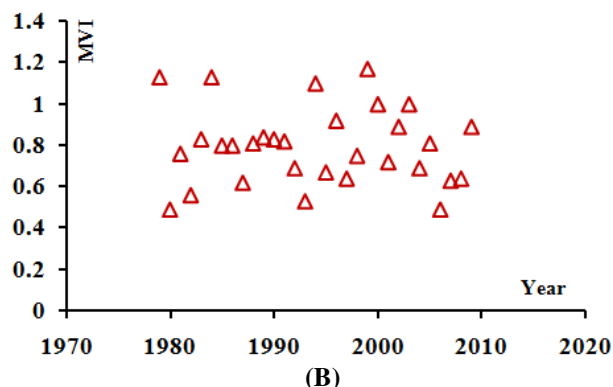


Fig. 16. Temporal variability of wave resources. A – Coefficient of Variation of Power; B – Monthly Variation Index.

**4.5 Representativeness of the output power from NC**

The energy from NC is a time-varying quantity. Thus, to estimate this parameter it is necessary to achieve the minimum sampling dimension to guarantee its temporal representativeness. As the wave regime is the only parameter that causes the variation in the energy content produced by NC, we assume that the minimum sampling size necessary to characterize the monthly average power on waves is equal to the minimum sampling size to characterize the monthly average power emanating from the NC. Further, this minimum sampling dimension is converted in numbers of days for monitoring the NC in order to achieve the temporal representativeness of the power data. In this way, using the Minitab software, the minimum number of sample points, for average monthly power, was calculated admitting a 0.85 power factor, a significance level equal to 0.05 and a value of 3kW/m for margin of error. This margin of error was assumed taking into account the possibility to completing all measurements in one year. In this context, lower margin of error implies higher number of sample points. Table 7 (appendix) show the standard deviations, the minimum sampling size to guarantee the representativeness of the values of the monthly average power and, consequently, the number of days to carry out the experiments on the NC in order to ensure the correct values of the average power extracted from these natural infrastructures. It is important to note that during the spring (March to May) and summer (June to August) the minimum numbers of days of measurements are lowers in comparison with the rest of the months. The reason for this finding is associated with the nature of the wave data for the referred months. That is, during the spring and

summer the wave data present low dispersion as it is possible to see through the values of the standard deviation in Table 7 (appendix), indicating that the wave energy resources are most stable during these periods of the year. Therefore, the minimum sample size for characterizing these wave data is lower than the rest of the months for which the standard deviations are higher.

**Table 7** :Minimum sampling size and the corresponding numbers of days of measurements

Power Factor: 0.85; Margin of Error: 3 kW/m; Significance level: $\alpha = 0.05$			
Months	Standard deviation, $\sigma$	Minimum sampling size, n	Numbers of days (for 3 h time step)
J	13.25	178	23
F	11.01	123	16
M	8.63	77	10
A	7.01	51	7
M	7.25	55	7
J	6.65	47	6
J	7.46	58	8
A	7.99	66	9
S	9.98	102	13
O	10.80	119	15
N	12.78	165	21
D	13.78	192	24

### 5 Conclusion

The most common sea state in Cape-Verde occurs 20.81% of time, featuring peak periods from 6-9 s and significant wave height from 1.5-2 m. For period between 1979 and 2009, 78.03% of the waves present wave height between 1 and 2 m. January and December are the most energetic months and July is the least energetic month. The monthly wave power decreases from January to July and increases again to December. Through the Coefficient of Variation of Power (COVP) it is possible to conclude that the wave resource is stable, with COVP between 0.46 and 0.66.

The MVI parameter shows that the wave resource can be considered relatively stable (MVI <1.2) from monthly average power point of view.

The time-series of annual-average wave power shows some attenuation over the years, due to the occurrence of effect of aggregation. However, using the smoothing moving average curve it is possible to verify that, from 1999, annual-average wave power oscillate around of 18kW/m.

This trend is continued in 10 years projected annual-average future values.

The outliers, present in time-series of annual-average power were identified and their influence in the value of annual-average power was quantified. Removing outliers from the annual time-series of power caused a maximum relative attenuation in the values of the annual-average power between 1.85 and 13%.

The minimum recording time of physical parameters associated with the NC operation are determined, for each month, under the assumption that the minimum sampling size necessary to characterize the monthly average power on waves is equal to the minimum sampling size to characterize the monthly average power emanating from the NC. In this context and for the Cape-Verde Wave Regime, the minimum sampling size and the corresponding numbers of days of measurements are given in Table 7. During the spring and summer the wave resources are more stable than the rest of the year and, therefore, the minimum numbers of day for monitoring the NC are lower, in comparison with the rest of period of time.

### 6 Acknowledgements

We are grateful to Jackson Augusto Léger Monteiro for his important contribution to the realization of this work.

### References

- [1] G. Boyle, Renewable Energy: Power for a Sustainable Future. *Oxford University Press, United Kingdom, 2004.*
- [2] ABP Marine Environmental Research Ltd., *Technical Report, Report No. R1106 prepared for the UK Department of Trade and Industry, 2004.*
- [3] L. Monfor, J. Goldsmith, And F. Jones, Ocean Energy Technology Readiness, Patent, Development Status and Outlook. *International Renewable Energy Agency (IRENA), Abu Dhabi, 2014.*



- [4] D. Magagna, Oscillating Water Column Wave Pump: A Wave Energy Converter for Water Delivery, *Doctoral Thesis, Faculty of Engineering and the Environment, University of Southampton, England, 2011.*
- [5] EMEC. : Wave Developers. <http://www.emec.org.uk/marine-energy/wave-developers>, 2014.
- [6] *Scottish Renewable: Marine Milestones Report. Scottish Renewables, Glasgow, 2014.*
- [7] JRC. Ocean Energy Database, 2014.
- [8] W.M.L Monteiro, and A.J.N.A. Sarmiento, Using the Natural Caves for Wave Energy Extraction: Modelling the Airflow through its Superficial Cavities using a Bidirectional Venturi Tube. *Proc. EWTEC'2015, Nantes, 2015.*
- [9] Electra, *Relatório de Contas 2012. Electra-Empresa de Electricidade e Água, Cabo-Verde, 2012.* <http://www.electra.cv/index.php/2014-05-20-15-47-04/relatorios-sarl>.
- [10] Selenec, *Rapport Annuel 2015, Selenec – Société Nationale d'Électricité du Sénégal, Senegal, 2015.*
- [11] GESTO, *Plano Energético Renovável Cabo-Verde. Gesto-Energy Solutions, Algés, Portugal, 2011.*
- [12] J.M.C. Carvalho, *Elaboration of Third International Conference on Sustainable Development in Small Island States in Development, United Nations Development Programme, National Report, Republic of Cape-Verde, 2013.*
- [13] DGE, *Direcção Geral de Energia: Plano Energético de Cabo-Verde, Governo de Cabo-Verde, 2009.*
- [14] S. Shalin, M. Sidenmark and T. Andersson, Evaluation of a Mechanical Power Smoothing System for Wave Energy Converters, *Proc. EWTE'2013, Aalborg, 2013.*
- [15] J.R. Chaplin, F.J. Farley, M.E. Prentice, R.C.T. Rainey, S.J. Rimmer, and A.T. Roach, Development of the ANACONDA all-Rubber WEC, *Proc. 7th European Wave and Tidal Energy Conference, Portugal, Porto, 2007.*
- [16] A.C. Mendes, And W.M.L. Monteiro, Performance Analysis of a model of OWC energy converter in non-linear waves *Proc. 7th European Wave and Tidal Energy Conference, Portugal, 2007.*
- [17] V.O. Mora-Figueroa, C.H. Olivares, B. Holmes, B. and A.M. O'Hagan, Sowfia – Streamlining of Ocean Wave Farms Impact Assessment, *Catalogue of Wave Energy Test Centres, IEE/09/809/SI2.558291, March, 2011.*
- [18] H.L. Tolman, User manual and system documentation of Wave Watch-III version 1.18, *OMB Technical Note 166, N.O.A.A, National Centre for Environmental Prediction, MD, USA, 1999.*
- [19] E.B.L. Mackay, A.S. Bahaj, and P.G. Challenor, Uncertainty in wave energy resource assessment. Part 2: Variability and predictability, *Renewable Energy, 35, 2010.*
- [20] G.J. Komen, I. Cavaleri, M. Donelan, K. Hasselmann, S. Hasselmann, and P.A.E.M. Janssen, Dynamics and modelling of ocean waves, *Cambridge University Press, Cambridge, 1994.*
- [21] NOAA, National Oceanic and Atmospheric Administration, *National Centers for Environmental Information, 2015 website: http://maps.ngdc.noaa.gov/viewers/bathymetry/*
- [22] S. Ponce de León, A.L. Silva and C. Guedes Soares, Reconstituição das Condições de Agitação Marítima no Arquipélago de Cabo-Verde, *IV Congresso sobre Planeamento e Gestão de Zonas Costeiras dos Países de Expressão Portuguesa, Portugal, 2010.*
- [23] R.G. Dean, and R.A. Dalrymple, Water Waves Mechanics for Engineers and Scientists, *World Scientific Pub. Co., Teaneck, NJ, 1991.*
- [24] G. Hagerman, Southern New England Wave Energy Resource Potential, *Proc. Building Energy'2001, Boston, USA, 2001.*
- [25] A.M. Cornett, A Global Wave Energy Resources Assessment, *Proc. International Journal of Offshore and Polar Engineering, Canada, 2008.*
- [26] P. Kuhnert, And W. Venables, An Introduction to R Software for Statistical Modeling and Computing, *CSIRO Mathematical and Information Science, Australia, 2005*
- [27] A. Cottrell, And R. Lucchetti, *gretl User's Guide, Winston-Salem, NC, URL http://Ricardo.ecn.wfu.edu/pub/gretl/manual/en/gretl-guide.pdf.*
- [28] XLSTAT, 2015 website: <https://www.xlstat.com/en/>
- [29] Minitab, Minitab 17 Statistical Software, *Minitab Inc., State College, Pennsylvania, USA, 2010.*
- [30] S. Bisgaard, and M. Kulahci, Time-series Analysis and Forecasting by Example, *John Wiley & Sons, Hoboken, New Jersey, 2011.*
- [31] L.H. Holthuijzen, Wave in Oceanic and Coastal Waters, *Delft University of Technology and UNESCO-IHE, Cambridge University Press, The Edinburgh Building, UK, 2007.*

- [32] E.G.G. Faria, J.A. Lorenzetti, and B. Chapron Swell and Wind-Sea Distribution Over the Mid-Latitude and Tropical North Atlantic for the Period 2002-2008, *International Journal of Oceanography*, volume 12, 2012.
- [33] H.B. Mann, Nonparametric Tests against Trend, *Econometrica*, Vol.13, No.3 1945.
- [34] R. J. Hyndmann, A.B. Koehler, J.K. Ord, and R.D. Snyder, Forecasting With Exponential Smoothing, *Springer-Verlag, Berlin, Heidelberg, 2008*.
- [35] G.W. Schwert, Tests for Unit Roots: A Monte Carlo Investigation, *Journal of Business and Economic Statistics*, 7, 1989.
- [36] H. Komm, Forecasting High-Frequency Volatility Shocks : An Analytical Real-time Monitoring System, *Springer Gabler, Catholic University Eichstatt-Ingolstadt, Germany, 2015*.
- [37] T. Stadnitski, Deterministic or Stochastic Trend: Decision on the Basis of the Augmented Dickey-Fuller Test, *Methodology European Journal of Research Methods for the Behavioral and Social Sciences* 6 (2), 2009.
- [38] W.A.V. Clark, and K.L. Avery, The Effects of data Aggregation in Statistical Analysis, *Geographical Analysis*, Vol.8, Issue 4, pages 428-438, 1976.
- [39] R. Johnson, Applied Multivariate Statistical Analysis, *Prentice Hall, 1992*.
- [40] R.B. D'Agostino, Test for Normal Distribution, Goodness-of-Fit Techniques, *D'Agostino, R.B. and Stephens, M.A., editors, New York, Marcel Dekker, ISBN 0-8247-7487-6, 1986*.
- [41] K.S. Kannan, K. Manoj, And S. Arumugan, Labeling Methods for Identifying Outliers, *International Journal of Statistics and Systems*, ISSN0973-2675, Vol.10, No. 2, 2015.
- [42] J. Frain, Lecture Notes on Univariate Time Series Analysis and Box Jenkins Forecasting, Economic Analysis, *Research and Publications, January 1999*
- [43] J.L. Hintze, *NCSS User's Guide IV*, Kaysville, Utah 84037, 2007.
- [44] J. Falnes, *A Review of Wave-Energy Extraction. Marine Structures* 20, 2007.
- [45] Jr. H.C. Thode, Testing for Normality, *State University of New York, Marcel Dekker, New York, 2002*.

## Appendix

Table 2: Histogram

		Peak Period, Tp[s]								Occurrence of Hs	%Occurrence of Hs
		1-3	3-6	6-9	9-12	12-15	15-18	18-21	21-24		
Significant Wave Height, Hs [m]	0-0.5	0	0	0	0	0	0	0	0	0	0.00
	0.5-1	1	3	170	427	141	29	6	0	777	0.86
	1-1.5	0	572	8307	9194	7288	1742	127	4	27234	30.07
	1.5-2	0	730	18854	7590	12783	3315	171	2	43445	47.96
	2-2.5	0	20	8482	2072	3329	1355	85	0	15343	16.94
	2.5-3	0	0	1657	731	431	293	25	0	3137	3.46
	3-3.5	0	0	254	219	51	47	7	0	578	0.64
	3.5-4	0	0	28	29	3	8	1	0	69	0.08
	>4	0	0	0	0	0	0	0	0	0	0.00
	Occurrence of Tp	1	1325	37752	20262	24026	6789	422	6	90583	100
%Occurrence of Tp	0.00	1.46	41.68	22.37	26.52	7.49	0.47	0.01	100		

Table 3: The Mann-Kendall Trend test for monthly average time-series.

Months	J	F	M	A	M	J	J	A	S	O	N	D
p-values	0.946	0.176	0.696	0.311	0.825	0.302	0.424	0.199	0.038	0.018	0.866	0.176
Decision	Without Trend	Without Trend	Without Trend	Without Trend	Without Trend	Without Trend	Without Trend	Without Trend	With Trend	With Trend	Without Trend	Without Trend

Table 4 : Energy use by suburb The AIC, BIC and HQC values as a function of Lag length, for annual-average power time-series.

Lags	1	2	3	4	5	6	7	8	9
AIC	3.23*	3.27	3.29	3.33	3.42	3.48	3.41	3.50	3.49
BIC	3.38*	3.47	3.54	3.63	3.76	3.88	3.86	3.99	4.03
HQC	3.27*	3.32	3.35	3.40	3.50	3.57	3.51	3.62	3.62

Table 5: Numbers of outliers present in each annual time-series of power.

Year	1979	1980	1981	1982	1983	1984	1985	1986	1987	1988	1989	1990	1991	1992	1993	1994	1995	1996	1997	1998	1999	2000	2001	2002	2003	2004	2005	2006	2007	2008	2009
No. of Outliers	130	132	151	120	111	146	102	107	104	92	155	125	110	124	128	114	95	149	149	78	134	106	124	118	187	95	31	134	101	108	180

Table 6: Monthly statistical reports Energy.

Variable	Simple size. N	Anderson-Darling Normality Test		Mean	StDev	SE Mean	95% CI
J	Hs[m]	7687	A-Squared: 40.63	p-value <0.005	1.92191	0.50899	0.00581 (1.91053; 1.93329)
	Tp[s]	7687	A-Squared: 170.24	p-value <0.005	10.7142	3.1631	0.0361 (10.6435; 10.7849)
	P [kW/m]	7687	A-Squared: 202.38	p-value <0.005	23.513	13.783	0.157 (23.205; 23.821)
F	Hs [m]	7008	A-Squared: 15.53	p-value <0.005	1.87711	0.46451	0.00555 (1.86623; 1.88798)
	Tp[s]	7008	A-Squared: 145.66	p-value <0.005	10.4387	3.0192	0.0361 (10.3680; 10.5094)
	P [kW/m]	7008	A-Squared: 208.03	p-value <0.005	21.897	12.716	0.152 (21.599; 22.195)
M	Hs [m]	7689	A-Squared: 21.63	p-value <0.005	1.80126	0.43902	0.00501 (1.79144; 1.81107)
	Tp[s]	7689	A-Squared: 70.03	p-value <0.005	10.8515	2.8814	0.0329 (10.7871; 10.9159)
	P [kW/m]	7689	A-Squared: 131.79	p-value <0.005	20.780	10.801	0.123 (20.538; 21.021)
A	Hs[m]	7440	A-Squared: 36.30	p-value <0.005	1.80543	0.38490	0.00446 (1.79668; 1.81417)
	Tp[s]	7440	A-Squared: 118.55	p-value <0.005	10.3233	2.7986	0.0324 (10.2597; 10.3869)
	P[kW/m]	7440	A-Squared: 161.64	p-value <0.005	19.763	9.983	0.116 (19.536; 19.990)

	<b>Hs[m]</b>	15376	A-Squared: 29.32	p-value <0.005	1.73386	0.31984	0.00258	(1.72881; 1.73892)
	<b>Tp [s]</b>	15376	A-Squared: 491.92	p-value <0.005	10.2287	3.0524	0.0246	(10.1804; 10.2769)
<b>M</b>	<b>P[kW/m]</b>	15376	A-Squared: 258.45	p-value <0.005	17.8068	7.9966	0.0645	(17.6804; 17.9332)
	<b>Hs[m]</b>	14880	A-Squared: 29.78	p-value <0.005	1.64809	0.30307	0.00248	(1.64322; 1.65296)
	<b>Tp [s]</b>	14880	A-Squared: 618.05	p-value <0.005	10.1125	3.0069	0.0246	(10.0642; 10.1608)
<b>J</b>	<b>P[kW/m]</b>	14880	A-Squared: 291.89	p-value <0.005	16.0597	7.4576	0.0611	(15.9399; 16.1795)
	<b>Hs[m]</b>	15376	A-Squared: 46.52	p-value <0.005	1.59065	0.26830	0.00216	(1.58640; 1.59489)
	<b>Tp [s]</b>	15376	A-Squared: 849.41	p-value <0.005	10.1592	2.8717	0.0232	(10.1138; 10.2046)
<b>J</b>	<b>P[kW/m]</b>	15376	A-Squared: 254.08	p-value <0.005	15.0375	6.6470	0.0536	(14.9324; 15.1425)
	<b>Hs[m]</b>	7688	A-Squared: 27.43	p-value <0.005	1.57631	0.26316	0.00300	(1.57043; 1.58219)
	<b>Tp[s]</b>	7688	A-Squared: 337.55	p-value <0.005	10.2906	2.9649	0.0338	(10.2243; 10.3569)
<b>A</b>	<b>P[kW/m]</b>	7688	A-Squared: 174.44	p-value <0.005	15.1119	7.2471	0.0827	(14.9499; 15.2740)
	<b>Hs[m]</b>	7440	A-Squared: 13.53	p-value <0.005	1.59887	0.27965	0.00324	(1.59251; 1.60522)
	<b>Tp[s]</b>	7440	A-Squared: 204.76	p-value <0.005	10.2960	2.8409	0.0329	(10.2315; 10.3606)
<b>S</b>	<b>P[kW/m]</b>	7440	A-Squared: 143.42	p-value <0.005	15.4316	7.0104	0.0813	(15.2723; 15.5910)
	<b>Hs[m]</b>	7687	A-Squared: 24.60	p-value <0.005	1.60069	0.33400	0.00381	(1.59322; 1.60816)
	<b>Tp[s]</b>	7687	A-Squared: 61.21	p-value <0.005	10.8908	2.8969	0.0330	(10.8261; 10.9556)
<b>O</b>	<b>P[kW/m]</b>	7687	A-Squared: 188.74	p-value <0.005	16.5502	8.6290	0.0984	(16.3573; 16.7431)
	<b>Hs[m]</b>	7440	A-Squared: 45.13	p-value <0.005	1.65678	0.39347	0.00456	(1.64784; 1.66573)
	<b>Tp[s]</b>	7440	A-Squared: 47.37	p-value <0.005	11.0808	2.9679	0.0344	(11.0133; 11.1482)
<b>Z</b>	<b>P[kW/m]</b>	7440	A-Squared: 212.76	p-value <0.005	18.439	11.008	0.128	(18.189; 18.689)
	<b>Hs[m]</b>	7688	A-Squared: 65.15	p-value <0.005	1.80871	0.45569	0.00520	(1.79852; 1.81890)
	<b>Tp[s]</b>	7688	A-Squared: 110.55	p-value <0.005	10.7810	3.1661	0.0361	(10.7102; 10.8518)
<b>D</b>	<b>P[kW/m]</b>	7688	A-Squared: 298.54	p-value <0.005	21.213	13.252	0.151	(20.917; 21.509)